Clinical Chemistry 67:3
534–542 (2021)

Giant Magnetoresistive Nanosensor Analysis of Circulating Tumor DNA Epidermal Growth Factor Receptor Mutations for Diagnosis and Therapy Response Monitoring

Jared C. Nesvet,[a] Katie A. Antilla,[b] Danielle S. Pancirer,[c] Alexander X. Lozano,[d,e] Jordan S. Preiss,[c] Weijie Ma,[f] Aihua Fu,[g] Seung-Min Park,[h,i] Sanjiv S. Gambhir,[h,i,j] Alice C. Fan,[k] Joel W. Neal,[c,k] Sukhmani K. Padda,[c,k] Millie Das,[c,k,l] Tianhong Li,[f] Heather A. Wakelee,[c,k] and Shan X. Wang[d,j,m,*]

BACKGROUND: Liquid biopsy circulating tumor DNA (ctDNA) mutational analysis holds great promises for precision medicine targeted therapy and more effective cancer management. However, its wide adoption is hampered by high cost and long turnaround time of sequencing assays, or by inadequate analytical sensitivity of existing portable nucleic acid tests to mutant allelic fraction in ctDNA.

METHODS: We developed a ctDNA *Epidermal Growth Factor Receptor* (EGFR) mutational assay using giant magnetoresistive (GMR) nanosensors. This assay was validated in 36 plasma samples of non-small cell lung cancer patients with known EGFR mutations. We assessed therapy response through follow-up blood draws, determined concordance between the GMR assay and radiographic response, and ascertained progression-free survival of patients.

RESULTS: The GMR assay achieved analytical sensitivities of 0.01% mutant allelic fraction. In clinical samples, the assay had 87.5% sensitivity (95% CI = 64.0—97.8%) for Exon19 deletion and 90% sensitivity (95% CI = 69.9—98.2%) for L858R mutation with 100% specificity; our assay detected T790M resistance with 96.3% specificity (95% CI = 81.7–99.8%) with 100% sensitivity. After 2 weeks of therapy, 10 patients showed disappearance of ctDNA by GMR (predicted responders), whereas 3 patients did not (predicted nonresponders). These predictions were 100% concordant with radiographic response. Kaplan-Meier analysis showed responders had significantly ($P < 0.0001$) longer PFS compared to nonresponders (N/A vs. 12 weeks, respectively).

CONCLUSIONS: The GMR assay has high diagnostic sensitivity and specificity and is well suited for detecting EGFR mutations at diagnosis and noninvasively monitoring treatment response at the point-of-care.

Introduction

Somatic mutations in the *Epidermal Growth Factor Receptor* (EGFR) gene confer sensitivity to tyrosine kinase inhibitors (TKIs) in non-small cell lung cancer (NSCLC) (1). Knowing the status of these activating mutations is critical for proper therapy selection, and personalized treatment based upon EGFR mutation status can improve progression-free survival (PFS) in these patients compared to standard chemotherapy (2). Two of the most prominent EGFR mutations—a deletion in exon 19 (Exon19 del) and a substitution in exon 21 (L858R)—are commonly treated with TKIs, including first-generation drugs erlotinib and gefitinib, and more recently with the third-generation agent osimertinib. While many patients initially exhibit favorable response to these therapies, a majority eventually develop resistance and progression (3). For ∼50% of patients treated with first-generation TKIs, resistance occurs via a secondary T790M mutation, which is resistant to first-

[a]Department of Chemistry, Stanford University, Stanford, CA, USA; [b]Department of Chemical Engineering, Stanford University, Stanford, CA, USA; [c]Stanford Cancer Institute, Stanford University School of Medicine, Stanford, CA, USA; [d]Department of Materials Science and Engineering, Stanford University, Stanford, CA, USA; [e]Faculty of Medicine, University of Toronto, Toronto, ON, Canada; [f]Department of Internal Medicine, Division of Hematology and Oncology, University of California Davis School of Medicine, University of California Davis Comprehensive Cancer Center, Sacramento, CA, USA; [g]Nvigen Inc, San Jose, CA, USA; [h]Department of Radiology, Stanford University School of Medicine, Stanford, CA, USA; [i]Molecular Imaging Program at Stanford, Stanford University School of Medicine, Stanford, CA, USA; [j]Canary Center at Stanford for Cancer Early Detection, Stanford University School of Medicine, Palo Alto, CA, USA; [k]Division of Oncology, Department of Medicine, Stanford University School of Medicine, Stanford, CA, USA; [l]VA Palo Alto Healthcare System, Department of Medicine, Palo Alto, CA, USA; [m]Department of Electrical Engineering, Stanford University, Stanford, CA, USA.
*Address correspondence to this author at: 476 Lomita Mall Room 351, Stanford, CA 94305, USA. Fax 1-650-736 1984; e-mail sxwang@stanford.edu.
Received July 15, 2020; accepted September 28, 2020.
DOI: 10.1093/clinchem/hvaa307

generation TKIs (4). The third-generation agent osimertinib is effective against Exon19 del, L858R, and the T790M mutation (5). Osimertinib showed both PFS and overall survival improvement compared to first-generation EGFR TKIs in the FLAURA study, thus patients with NSCLC in the U.S. are now being treated first-line with osimertinib (6). However, from a global health perspective, third-generation TKIs are cost-prohibitive in some countries in eastern Asia – where the prevalence of EGFR mutations is approximately double that of the U.S. population (7)—necessitating the need for surveillance of T790M mutation for timely changing of therapeutic regiment, if necessary, for those treated with first-generation medications. Despite the success of targeted EGFR inhibitors, it is estimated that 20% of lung cancer patients begin therapy prior to EGFR testing (8), for reasons such as inability to biopsy certain patients, and long turnaround times to results. Clearly, new technologies for mutational analysis that are highly sensitive, yet affordable, noninvasive, and with fast turnaround are needed.

Liquid biopsy, or blood-based detection of biomarkers, has emerged as a noninvasive alternative diagnostic for a variety of applications (9–11). Specifically in cancer, solid tumors shed numerous biomarkers into the vasculature, including circulating tumor DNA (ctDNA) (12, 13). Because ctDNA originates from primary and metastatic tumor sites, it can be used as a proxy for genetic information, and there is a strong concordance between tissue mutational status reflected in blood biomarkers (14, 15). Tissue biopsy can suffer from sampling bias and intratumoral heterogeneity, which can lead to false negatives (16); ctDNA as a companion diagnostic for tumor genomic profiling overcomes these issues for treatment selection. In addition to genomic profiling for initial therapy selection, ctDNA is particularly well suited for monitoring therapy response and development of resistance (17–20). Unlike tissue biopsy or radiographic imaging, it is possible to sample patients by liquid biopsy frequently for dynamic measurement of response or subclonal evolution of resistant mutations (8). Studies have shown loss of ctDNA in the bloodstream is indicative of a favorable response to therapy (21, 22), and dynamic measurement of ctDNA clearance could be prognostic of relapse (23). However, ctDNA comprises a small fraction of total cell-free DNA (cfDNA), as little as 0.1% (24), necessitating extremely sensitive tests for ctDNA.

Common technologies for ctDNA genomic profiling in the clinic include amplification-refractory mutation system (ARMS)-PCR assays with fluorescent Taqman probes, digital methods such as beads, emulsion, amplification, and magnetics (BEAMing) or droplet digital PCR (ddPCR), and next generation sequencing (NGS) assays. Two ARMS-PCR assays are FDA approved; they have inexpensive reagent costs, low technical requirements, and fast turnaround time. However, these fluorescent assays generally have lower analytical and clinical sensitivities (75–100 copies/mL and 70% sensitivity, respectively) (23, 25). Digital PCR has enhanced sensitivity compared to ARMS-PCR assays but limited multiplexing capability and requires specialized equipment for partitioning sample into individual droplets (26). NGS assays have the benefit of high sensitivities (0.1–0.01% mutant allelic fractions) and multiplexability (27, 28), but are more expensive and require advanced technical skills and instrumentation that may not be present in the clinic, thus samples are often sent to a central facility for processing and can sometimes take 2 or more weeks for results. Giant magnetoresistive (GMR) nanosensors retain advantages from both technologies – they have extremely high sensitivity and multiplexability, but retain low costs and rapid testing time. Magnetic detection of biomolecules such as proteins (29–33) and DNA (34–37) via GMR sensors is due to a change in resistance in the magnetic stack structure of the nanosensor when the local magnetic field is altered due to magnetic nanoparticle binding to biofunctionalized sensors (Fig. 1). We previously reported on the development of GMR nanosensor technology for the detection of mutations and differential methylation using cancer cell lines for assay optimization; our sensitivity ranged from 10% mutant allelic fraction (38) to 0.1% methylated allelic fraction upon the addition of a biased PCR amplification (39). Here, we report that GMR assay analytical sensitivity can reach 0.01% mutant allelic fraction in clinical ctDNA samples, and the clinical translation of GMR nanosensors to detect ctDNA in patient plasma for targeted therapy monitoring and prognosis.

Materials and Methods

PATIENT ENROLLMENT AND SAMPLE PROCESSING

Thirty patients were consented and enrolled at either Stanford University Medical Center or the University of California, Davis under IRB-21319 and IRB-226210 (Supplemental Table 1). Blood was collected from patients in a 10 mL K_2-EDTA blood tube and was kept at 4 °C until processing. Plasma was separated from whole blood within 2 h of sample collection by two cycles of centrifugation at 1250 *g* for 12 min. The plasma was then stored at -80°C in a 15 mL Falcon tube until further processing. Cell-free DNA was extracted from 1.5–3 mL of plasma using the MagVigen Plasma DNA Capture kit (Nvigen). Total cfDNA concentration was quantified using the Qubit dsDNA HS Assay kit (ThermoFisher).

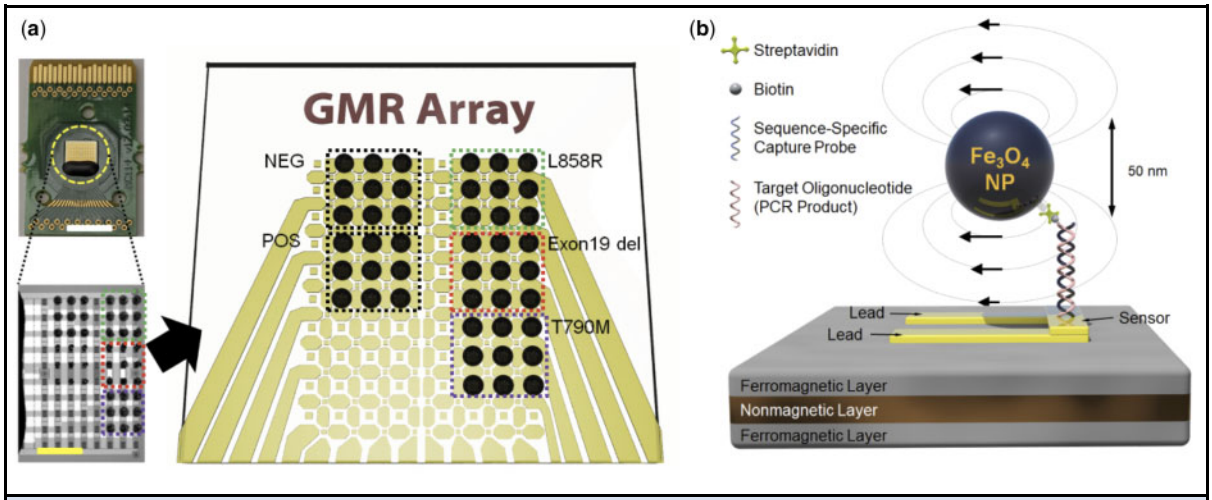

Fig. 1. a) GMR sensor chip (top left, scale = 5 mm) with expanded view of 8 x 10 GMR sensor array (bottom left, scale = 0.5 μm) and rendering of 9 functionalized sensors per target (right); b) rendering of nanosensor magnetic stack structure with nanoparticle binding through biotin-streptavidin interaction with hybridized PCR product (note figure not drawn to actual scale).

CELL LINE DNA AND HEALTHY WHITE BLOOD CELL DNA EXTRACTION

Cell lines were obtained from the American Type Culture Collection (ATCC). NCI-H1975 (ATCC CRL-5908) and HCC827 (ATCC CRL-2868) were cultured in RPMI-1640 medium containing 10% fetal bovine serum and antibiotics at 37 °C and 5% CO_2. Genomic DNA was isolated using the Qiagen Blood & Cell Culture DNA Kit, Genomic-tip 100/G (Qiagen GmbH, Hilden, Germany) and quantified using the Qubit dsDNA HS Assay kit (ThermoFisher Scientific, Waltham, MA). Alternative DNA extraction using Micrococcal Nuclease (MNase) was also performed on both cell lines using the EZ Nucleosomal DNA Prep Kit (Zymo Research, Irvine, CA). Micrococcal nuclease-treated DNA concentration was quantified using the Qubit dsDNA HS Assay kit, and the fragmentation pattern was analyzed using the Agilent 2100 Bioanalyzer. Healthy whole blood was collected from the Stanford Research Blood Bank, and genomic DNA was collected using the Qiagen Blood & Cell Culture DNA Kit, Genomic-tip 100/G.

PCR AMPLIFICATION

All oligonucleotides were purchased from Integrated DNA Technologies. PCR amplification was performed with BioRad SsoAdvanced Universal SYBR Green Supermix. PCR was performed using 10 μL supermix, with primer concentrations of 0.25 μM (L858R/T790M) and 0.5 μM (Exon19 del), and blocker concentrations of 1 μM (L858R/T790M) and 2 μM (Exon19 del), for a total volume of 20 μL (Supplemental Table 2). Reaction conditions were as follows: 95 °C for 3 min, followed by 35 cycles of 95 °C for 10 sec and 62.5 °C for 30 sec. For patient samples, PCR was performed in duplicate, with 7 μL of cfDNA per reaction; additionally, a 30 ng white blood cell genomic DNA wild-type control to account for nonspecific amplification and a no template control to account for contamination were run with each PCR reaction.

GMR ASSAY PROCESSING

The GMR biosensor chip has a multilayer spin valve structure fabricated in an 8 x 10 array, as described previously (32). GMR sensors (n = 9 per mutation) were functionalized with single-stranded hybridization probes complementary to their respective EGFR target (Supplemental Table 2) using standard (3-aminopropyl)triethoxysilane and glutaraldehyde surface chemistry (39).

The PCR product was analyzed on GMR sensors as follows: The functionalized GMR chip was blocked with 1% w/w bovine serum albumin (BSA) in phosphate buffered saline (PBS) for 1 h, then washed with distilled water. 10 μL of PCR product was diluted in 140 μL of hybridization buffer (400 mM NaCl in Tris-EDTA buffer, ThermoFisher), denatured at 95 °C for 10 min, and cooled on ice for 5 min. The PCR product was hybridized on the GMR chip at 37 °C for 1 h. The chip was washed 6x with denaturation buffer (10 mM NaCl in Tris-EDTA buffer) at 4 °C. Each chip was mounted in a GMR reading station and a baseline signal was recorded for 1 min. 50 μL of Streptavidin MACS (Miltenyi) magnetic nanoparticles (MNPs) were added

and the GMR signal was measured in parts per million (ppm) for 15 min. PCR duplicates for each patient were measured on separate chips. Signal background correction included: 1) removing sensors with signal outside 2σ of the mean GMR signal, 2) subtracting median negative reference signal, 3) calculating the mean GMR signal of each duplicate, and 4) subtracting median white blood cell GMR signal for each mutation. Single-use GMR chips were used for each patient sample and the negative controls were used to assess carryover contamination, if any, of PCR products.

STATISTICAL METHODS

A Mann-Whitney *U*-test was used because of our sample cohort size (n = 36) as it does not assume normal distribution when comparing independent groups. ROC curves were generated with GraphPad Prism8, thresholds were selected with the highest Youden's J statistic. The Kaplan-Meier method was used for evaluating PFS, comparisons between groups were performed with the log-rank test. All statistical tests were 2-sided, and *P* values less than 0.05 were considered significant.

Results

ANALYTICAL SENSITIVITY OF GMR ASSAY AND cfDNA EXTRACTIONS

To determine the analytical sensitivity of the PCR/GMR portions of the assay, genomic DNA (gDNA) extracted from HCC827 (Exon19 del) and H1975 (L858R/T790M) cell lines was diluted into white blood cell gDNA (all wild-type). We created mixtures of 100%, 10%, 1%, 0.1%, 0.01%, and 0% mutant allelic fraction (MAF) with 30 ng total DNA, the mean expected value of cfDNA from 3 mL of plasma. The mixtures were PCR amplified, and the product was analyzed on the GMR sensors (Fig. 2, Supplemental Table 3). Using twice the standard deviation (σ) of the 0% GMR signal as background, the assay has a limit of detection (LoD) of 0.01% MAF for all 3 mutations; this is the equivalent of 1 mutant copy (3 pg DNA) in a background of 10,000 wild-type copies (30 ng DNA).

To determine the limit of detection (LoD) of the assay including the cfDNA extraction, MNase-fragmented DNA was used to generated contrived plasma samples, which closely resembled the nucleosomal fragmentation pattern of patient ctDNA. MNase-DNA was titrated into 3 mL of healthy plasma, the LoD of the assay was defined as the minimum amount of DNA that generated GMR signal significantly above (2σ) the GMR signal for zero analyte. The LoD for Exon19 del and L858R was 7 copies/mL, and the LoD for T790M was 25 copies/mL (Supplemental Fig. 1).

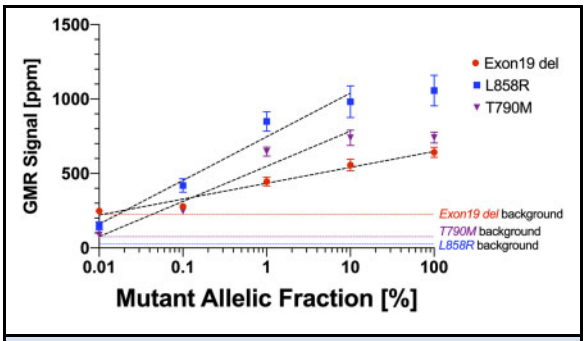

Fig. 2. Multiplexed GMR standard curves for Exon19 del, L858R, and T790M mutation dilution series, with total DNA weight of 30 ng. Background signal was defined as 2σ of the median GMR signal of 0% MAF for each mutation.

DETECTION OF "HOT SPOT" EGFR MUTATIONS IN PLASMA ctDNA BY GMR IN PATIENTS WITH METASTATIC NON-SMALL CELL LUNG CANCER

Thirty-six plasma samples were collected from 30 patients with metastatic NSCLC from 2 medical centers, Stanford University and University of California, Davis. All patients had $EGFR^+$ mutation confirmed by tumor tissue genomic profiling or commercial plasma ctDNA NGS assay (Supplemental Table 1). 1.5–3 mL of plasma was processed for each patient; a positive control of healthy plasma spiked with 5 ng of H1975/HCC827 gDNA and a negative control of healthy plasma were processed with each batch. The median cfDNA concentration, measured by Qubit, for cancerous patients was 11.3 ng/mL and for healthy controls was 6.55 ng/mL ($P = 0.001$). The patient GMR signals for the 3 "hot spot" mutations are shown in Fig. 3, and classified as mutant type or wild-type. A Mann-Whitney *U*-test was performed to compare median GMR signals between patients with mutant type and wild-type tumoral genotypes for all mutations, and were found to be statistically significant ($P < 0.0001$). The positive controls were utilized to determine the inter-assay coefficient of variance for each run, and for each mutation the coefficient of variance was <20% (Supplemental Fig. 2).

Receiver operating characteristic (ROC) curve analysis (Supplemental Fig. 3) was used to evaluate the clinical sensitivity and specificity of the GMR assay. For Exon19 del, the area under the ROC curve (AUC) was 0.953 (95% CI = 0.877–1.00) with an optimized sensitivity of 87.5% (95% CI = 64.0–97.8%) and 100% specificity (95% CI = 83.9–100%) using a signal of 10 ppm or higher as a positive result. For L858R, the AUC was 0.981 (95% CI = 0.946–1.00) and classifying any signal of 50 ppm or higher as a positive result

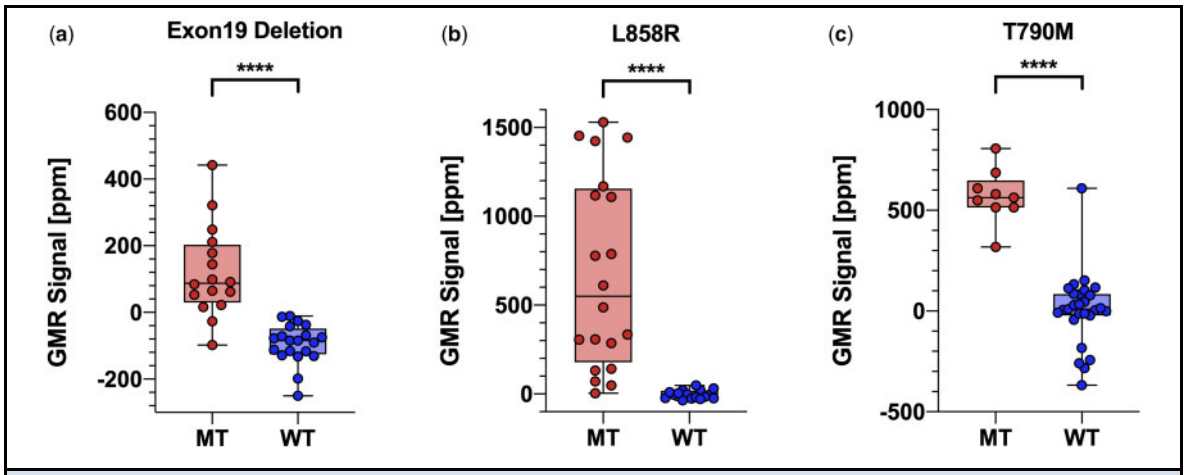

Fig. 3. Box and whisker plot for a) Exon19 del, b) L858R, and c) T790M background-corrected GMR signals. Due to negligent Exon19 del and T790M raw GMR signal, background correction with WBC DNA yielded negative GMR signal. Mann-Whitney *U*-test shows median GMR signal between patients with mutant type (MT) and wild-type (WT) tumors is statistically significant ($P < 0.0001$).

gave 90% sensitivity (95% CI = 69.9–98.2%) and 100% specificity (95% CI = 80.6–100%). T790M ROC curve analysis optimized for a sensitivity of 100% (95% CI = 70.1–100%) and specificity of 96.3% (95% CI = 81.7–99.8%) using a signal threshold of 300 ppm, with an AUC of 0.971 (95% CI = 0.914–1.00). All ROC curves were statistically significant ($P < 0.0001$).

MONITORING PATIENT RESPONSE TO TKI THERAPY

Thirteen patients received 2 follow-up (FU) blood draws after initiating TKI treatment, the first (FU1) ~2 weeks after beginning treatment, and the second (FU2) ~2–3 months after beginning treatment, which coincided with imaging of the tumor by CT. All patients received first-line osimertinib therapy. Patients were classified as either "responder" or "nonresponder" solely based upon GMR results from the FU1 draw at ~2 weeks. If a patient showed disappearance of mutational burden at FU1 (GMR signal below 10 ppm for Exon19 del or 50 ppm for L858R) this individual was classified as a responder, and if there was still evidence of mutation, the individual was classified as a nonresponder. Ten patients were classified as responders and 3 were nonresponders; GMR results of therapy response are shown in Fig. 4. While nonresponders did show a decrease in GMR signal at FU1, it still remained above the established thresholds. All responders maintained an absence of mutational GMR signal at FU2.

Radiographic response, measured by computed tomography (CT) imaging after 2–3 months of TKI therapy, for these 13 patients was evaluated by a physician as favorable response (FR), stable disease (SD), or progression of disease (PD). Classification of FR or SD was characterized by a clinically significant shrinkage of tumor volume or arrested growth in CT scan, respectively. PD classification was characterized as clinically significant growth of tumor volume. The FR, SD, and PD classifications were utilized because they were more relevant in clinical practice compared to RECIST v1.1 criteria. Five patients were classified FR, 5 patients were classified SD, and 3 patients were classified PD. The 3 PD patients were the same 3 who were classified as nonresponders by GMR analysis at 2 weeks.

Figure 5 shows the correlation between GMR results and clinical outcome for 2 representative patients. Figure 5, a shows results for Patient 20 who was classified as a nonresponder by GMR testing and radiographically exhibited PD; upon evidence of radiographic progression after 3 months, Patient 20 discontinued osimertinib and began combination platinum-doublet, antivascular endothelial growth factor, antiprogrammed death-ligand 1 immunotherapy, and radiotherapy, which stabilized thoracic disease. Figure 5, b shows results for Patient 12 who was classified as a responder by GMR testing and showed stable disease in CT imaging; this patient continued on osimertinib regimen. Overall, predictions of patient response by the GMR assay after only 2 weeks of TKI therapy were 100% concordant with radiographic outcome after ~2 months of TKI therapy—all patients predicted to be responders by the GMR assay displayed either FR or SD, and all nonresponders predicted by the GMR assay showed PD by CT imaging. Additionally, a retrospective set of longitudinal samples from a patient diagnosed with Exon19 del^{+}

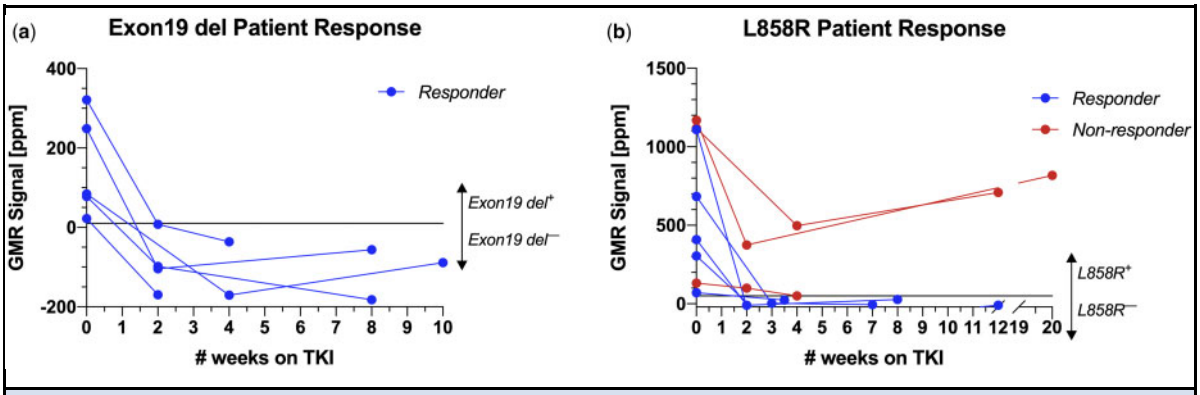

Fig. 4. GMR results for patient therapy monitoring with a) Exon19 del$^+$ and b) L858R$^+$ tumors. Black lines represent GMR signal thresholds determined by ROC analysis, 10 ppm and 50 ppm, respectively. Responders, shown in blue, are characterized by GMR signal below the threshold at first follow-up. Nonresponders, shown in red, are characterized by GMR signal above the threshold at first follow-up.

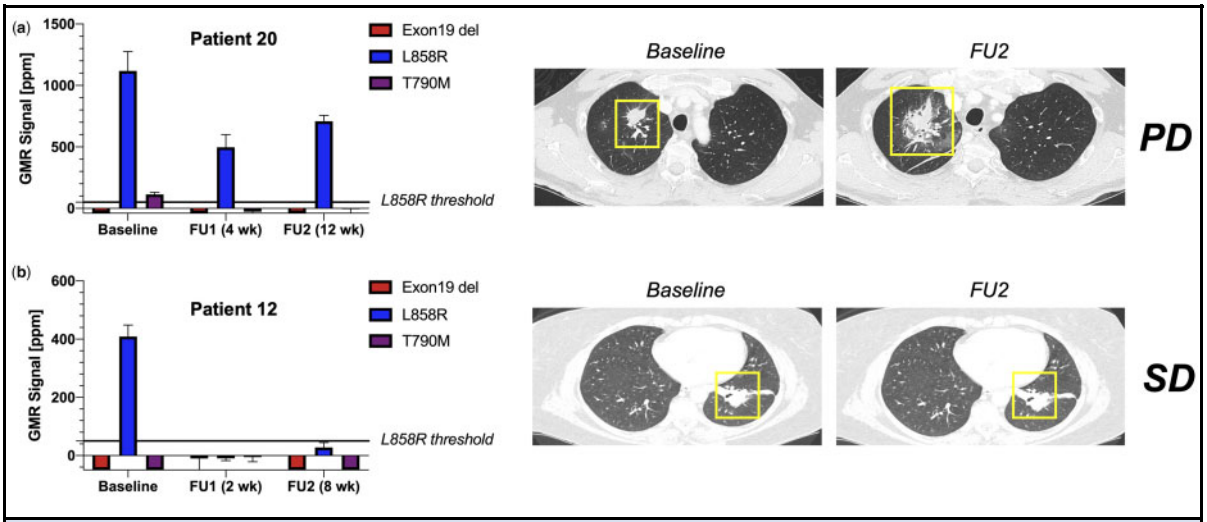

Fig. 5. Comparison of GMR signal to CT images. a) Patient 20 was a nonresponder by GMR testing. The CT image at FU2 shows significant tumor growth (PD); b) Patient 12 was a responder by GMR testing, and CT imaging shows no significant change in tumor size (SD).

tumor was collected over a 9-month period of erlotinib treatment, and the GMR assay was able to detect emergence of secondary T790M mutation as well (Supplemental Fig. 4).

RAPID PREDICTION OF LONGITUDINAL RESPONSE

We also used the GMR assay to ascertain progression-free survival (PFS) stratified by GMR responders ($N = 10$) versus nonresponders ($N = 3$) using the Kaplan-Meier method. PFS was measured by the number of weeks until radiographic progression from the initiation of TKI therapy or censor at the latest follow-up appointment (Fig. 6). GMR nonresponders had a median PFS of 12 weeks, whereas only 3 of 10 responders progressed, the rest had no progression at latest CT imaging (times of censor range from 32—49 weeks, median 37 weeks); hazard ratio (HR) for disease progression was 0.089 (95% CI = 0.0047–1.65). A median PFS for responders had not been reached, as 7 of 10 were censored prior to progression, but the survival curves are significantly different ($P < 0.0001$).

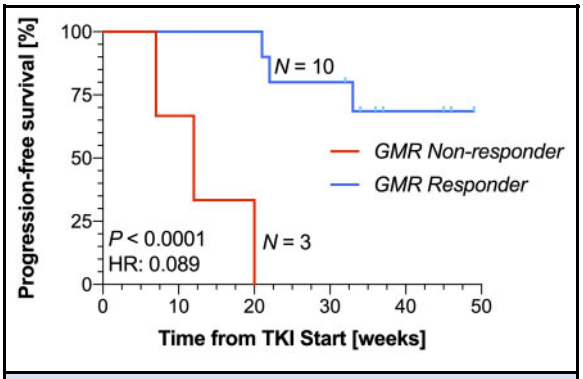

Fig. 6. Progression-free survival for responders vs. nonresponders identified by GMR assay. Progression was classified by clinically significant growth of tumor by CT scan.

Discussion

Many different tests for ctDNA EGFR genomic profiling exist for patients with NSCLC. In deciding which test to implement, clinical sensitivity and specificity are two important parameters to consider. However, other factors such as cost, turnaround time, and accessibility for those in resource-poor settings must also be taken into consideration. Compared to other fluorescent ARMS-PCR ctDNA tests, the GMR assay achieved lower analytical limits of detection (0.01% for all 3 mutations), which led to improved clinical sensitivities. Additionally, the GMR assay achieved comparable performance for the detection of common EGFR mutations compared to digital PCR methods in the literature (26). Utilizing novel nanoparticle-based technologies for cfDNA extraction and GMR detection of rare mutant alleles helped to improve performance of our assay. The cfDNA extraction used MNPs engineered for higher cfDNA extraction yield, and showed improved assay performance compared to a filter-based cfDNA extraction method in aliquoted patient samples (Supplemental Fig. 5). Improved assay sensitivity was also possible due to the higher signal-to-noise ratios when utilizing GMR nanosensors for detection compared to fluorescent detection (Supplemental Fig. 6). While the high sensitivities and specificities of this assay are promising, future testing on a larger cohort consisting of both test and validation sets, with equivalent numbers of L858R and Exon19 del samples, is needed to prove clinical utility for adoption in clinical practice.

For ROC curve analysis, we prioritized diagnostic specificity for primary somatic mutations (Exon19 del and L858R) but diagnostic sensitivity for secondary T790M mutation when determining GMR thresholds to separate positive and negative results. High specificity is important for detecting primary somatic mutations due to the adverse outcome of false positives: patients with tumors that are EGFR wild-type, but receive a false positive result would receive an ineffective TKI treatment. At 100% specificity, we were still able to achieve high sensitivity for Exon19 del and L858R mutations (87.5% and 90%, respectively). Given the equivalent analytical sensitivities for Exon19 del and L858R, we believe the differences in sensitivity are solely due to differences in sample size for patients with tumors harboring Exon19 del versus L858R mutation. For T790M diagnosis, we optimized for high sensitivity since the majority of patients develop T790M mutation as a secondary mutation while receiving first-generation TKIs. For the T790M mutation, a false negative result could be harmful because the patient would continue to receive therapy to which they have developed resistance, rather than switch to third-generation osimertinib that is effective against T790M. For T790M, we achieved 100% sensitivity while retaining high specificity as well (96.3%). Notably, the GMR assay detected the emergence of secondary T790M resistance in serial sampling of a patient with an initial Exon19 del mutation. Detection of T790M resistance is particularly important with the GMR assay, since patients most likely to develop T790M mutations are those in areas where first-line first-generation TKIs are still utilized, which may be in resource-poor settings where the benefits of the GMR assay are most apparent (lower cost, portability). The GMR assay is also well suited for monitoring of therapy response on a frequent weekly-to-monthly basis. While NGS assays are highly sensitive for rare mutant alleles in cfDNA, they become cost-prohibitive with frequent testing, and many assays have turnaround times of 2 weeks or longer. The GMR assay does not require batch storage and processing for cost savings (Supplemental Table 4 for cost analysis), meaning physicians can receive results within a day of sample collection and receive real-time insight into tumor dynamics. This is particularly important at first diagnosis.

The GMR assay can also be a useful complementary tool for assessment of therapy response by CT imaging. For some patients with NSCLC, including in this study, imaging can be ambiguous for assessment of patient response, even after 2–3 months of therapy. An SD classification can leave physicians uncertain whether their patient is actually responding to the therapy, and the future course of action is unclear. The decision to switch therapies is often delayed until future scans are more definitive, but this delay could potentially be harmful to a nonresponsive patient whose outcome is not clearly reflected in the CT scan. All patients with stable disease were responders by the GMR assay. A multimodality assessment of therapy response combining ctDNA GMR assay with imaging could resolve these issues and provide real-time information in

between CT scans, as ctDNA testing can be performed more often, to allow physicians to make more informed decisions and switch therapies much earlier if evidence of resistance appears.

After just 2 weeks of TKI therapy, the GMR assay offered rapid predictions of response. It accurately identified responders and nonresponders, and also offered prognostic assessment of PFS, which can help physicians identify patients to closely monitor those who will benefit from a quicker therapy change. For example, 3 months after beginning osimertinib therapy, Patient 20 exhibited radiographic disease progression and subsequently switched to standard chemotherapy in combination with monoclonal antibody therapy and radiotherapy, with much better response. However, 2 months prior to follow-up CT imaging, the GMR assay indicated Patient 20 had not responded to osimertinib initially; use of the GMR assay could have instigated this beneficial switch in therapy sooner. There is evidence in the literature that ctDNA as a biomarker for therapy response may be more sensitive and present earlier than radiographic progression (40), and while Patient 20 is one example, our GMR assay is a cost-effective but highly sensitive technology that could allow for frequent sampling for earlier detection of nonresponse and disease recurrence. The GMR assay could theoretically even allow for much longer intervals between imaging if the assay does not detect any evidence of loss of response. One limitation of our study of therapy response monitoring is the short time horizon for patient outcome. While all identified nonresponders had progressed in the current time horizon, the PFS data is not relatively mature—most responders were censored in this current study. A follow-up study using an expanded cohort and longer time horizon would allow continued assessment of PFS and OS from our GMR assay.

Nonstandard Abbreviations: TKIs, Tyrosine kinase inhibitors: TKIs; ctDNA, Circulating tumor DNA: ctDNA; cfDNA, Cell-free DNA: cfDNA; GMR, Giant magnetoresistive; ARMS-PCR, Amplification refractory mutation system PCR; BEAMing PCR, beads, emulsion, amplification, and magnetics PCR; ddPCR, Droplet digital PCR.

Human Genes: EGFR, Epidermal Growth Factor Receptor.

Author Contributions: *All authors confirmed they have contributed to the intellectual content of this paper and have met the following 4 requirements: (a) significant contributions to the conception and design, acquisition of data, or analysis and interpretation of data; (b) drafting or revising the article for intellectual content; (c) final approval of the published article; and (d) agreement to be accountable for all aspects of the article thus ensuring that questions related to the accuracy or integrity of any part of the article are appropriately investigated and resolved.*

S.X. Wang, H.A. Wakelee, T. Li, S.S. Gambhir, A.C. Fan, J.W. Neal designed research study, H.A. Wakelee, J.W. Neal, T. Li, S.K. Padda, and M. Das were physicians overseeing patient care, J.C. Nesvet, K.A. Antilla, A. Fu helped assay optimization, J.C. Nesvet, K.A. Antilla, A.X. Lozano helped collect and process patient samples, D.S. Pancirer, J.S. Preiss, W. Ma helped recruit and consent patients and coordinate samples, J.C. Nesvet, S.-M. Park, S.X. Wang, H.A. Wakelee, T. Li helped analyze research and write manuscript.

Authors' Disclosures or Potential Conflicts of Interest: *Upon manuscript submission, all authors completed the author disclosure form. Disclosures and/or potential conflicts of interest:*

Employment or Leadership: Aihua Fu, CEO of Nvigen Inc., which manufactured the cfDNA extraction kits; S.X. Wang, MagArray, Inc.
Consultant or Advisory Role: S.S. Gambhir, MagArray, Inc.; S.K. Padda, G1 Therapeutic, ASTRAZENECA, Pfizer, Blueprint; T. Li, Foundation Medicine, Inc, Archer Diagnostic; S.X. Wang, Nvigen Inc.
Stock Ownership: S.S. Gambhir, MagArray, Inc.; Aihua Fu, Nvigen Inc.; S.X. Wang, Nvigen, Inc., stock or stock options in MagArray, Inc., which has licensed relevant patents from Stanford University for commercialization of GMR nanosensor chips.
Honoraria: S.K. Padda, PER, CME solutions; M. Das, Astra Zeneca.
Research Funding: This work was supported by National Cancer Institute through Center for Cancer Nanotechnology Excellence on Translational Diagnostics (CCNE-TD, U54CA199075), the University of California Cancer Research Coordinating Committee grant 3-444964-34912, the Personalized Cancer Therapy Gift Fund (T. Li). T. Li, grants from Pfizer, Merck & Co., Hengrui Therapeutics, Inc., Eureka Therapeutics, Inc., and LabyRx Immunologic Therapeutics; J.W. Neal, research funding from Genentech/Roche, Merck.
Expert Testimony: None declared.
Patents: Aihua Fu, PCT/US35066; S.X. Wang, related patents or patent applications assigned to Stanford University and out-licensed for potential commercialization.
Other Remuneration: T. Li, personal fees from Foundation Medicine and Archer Diagnostics outside the submitted work.

Role of Sponsor: The funding organizations played no role in the design of study, choice of enrolled patients, review and interpretation of data, preparation of manuscript, or final approval of manuscript.

References

1. Taron M, Ichinose Y, Rosell R, Mok T, Massuti B, Zamora L, et al. Activating mutations in the tyrosine kinase domain of the epidermal growth factor receptor are associated with improved survival in gefitinib-treated chemorefractory lung adenocarcinomas. Clin Cancer Res 2005;11:5878–85.
2. Mok TS, Wu Y-L, Thongprasert S, Yang C-H, Chu D-T, Saijo N, et al. Gefitinib or carboplatin–paclitaxel in pulmonary adenocarcinoma. N Engl J Med 2009;361:947–57.
3. Wu Y-L, Zhou C, Hu C-P, Feng J, Lu S, Huang Y, et al. Afatinib versus cisplatin plus gemcitabine for first-line treatment of Asian patients with advanced non-small-cell lung cancer harbouring EGFR mutations (LUX-Lung 6): an open-label, randomised phase 3 trial. Lancet Oncol 2014;15:213–22.
4. Kobayashi S, Boggon TJ, Dayaram T, Jänne PA, Kocher O, Meyerson M, et al. EGFR mutation and resistance of non–small-cell lung cancer to gefitinib. N Engl J Med 2005;352:786–92.
5. Cross DAE, Ashton SE, Ghiorghiu S, Eberlein C, Nebhan CA, Spitzler PJ, et al. AZD9291, an irreversible EGFR TKI, overcomes T790M-mediated resistance to EGFR inhibitors in lung cancer. Cancer Discov 2014;4:1046–61.

6. Soria J-C, Ohe Y, Vansteenkiste J, Reungwetwattana T, Chewaskulyong B, Lee KH, et al. Osimertinib in untreated EGFR-mutated advanced non–small-cell lung cancer. N Engl J Med 2018;378:113–25.
7. Rosell R, Moran T, Queralt C, Porta R, Cardenal F, Camps C, et al. Screening for epidermal growth factor receptor mutations in lung cancer. N Engl J Med 2009;361: 958–67.
8. Reckamp KL, Melnikova VO, Karlovich C, Sequist LV, Camidge DR, Wakelee H, et al. A highly sensitive and quantitative test platform for detection of NSCLC EGFR mutations in urine and plasma. J Thorac Oncol 2016; 11:1690–700.
9. Lo YMD, Corbetta N, Chamberlain PF, Rai V, Sargent IL, Redman CW, et al. Presence of fetal DNA in maternal plasma and serum. Lancet 1997;350:485–7.
10. Moding EJ, Diehn M, Wakelee HA. Circulating tumor DNA testing in advanced non-small cell lung cancer. Lung Cancer 2018;119:42–7.
11. Rolfo C, Mack PC, Scagliotti GV, Baas P, Barlesi F, Bivona TG, et al. Liquid biopsy for advanced non-small cell lung cancer (NSCLC): a statement paper from the IASLC. J Thorac Oncol 2018;13:1248–68.
12. Jahr S, Hentze H, Englisch S, Hardt D, Fackelmayer FO, Hesch R-D, et al. DNA fragments in the blood plasma of cancer patients: quantitations and evidence for their origin from apoptotic and necrotic cells. Cancer Res 2001; 61:1659–65.
13. Oxnard GR, Paweletz CP, Kuang Y, Mach SL, O'Connell A, Messineo MM, et al. Noninvasive detection of response and resistance in EGFR-mutant lung cancer using quantitative next-generation genotyping of cell-free plasma DNA. Clin Cancer Res 2014;20:1698–705.
14. Newman AM, Bratman SV, To J, Wynne JF, Eclov NCW, Modlin LA, et al. An ultrasensitive method for quantitating circulating tumor DNA with broad patient coverage. Nat Med 2014;20:548–54.
15. Newman AM, Lovejoy AF, Klass DM, Kurtz DM, Chabon JJ, Scherer F, et al. Integrated digital error suppression for improved detection of circulating tumor DNA. Nat Biotechnol 2016;34:547–55.
16. Gerlinger M, Rowan AJ, Horswell S, Larkin J, Endesfelder D, Gronroos E, et al. Intratumor heterogeneity and branched evolution revealed by multiregion sequencing. N Engl J Med 2012;366:883–92.
17. Chabon JJ, Simmons AD, Lovejoy AF, Esfahani MS, Newman AM, Haringsma HJ, et al. Circulating tumour DNA profiling reveals heterogeneity of EGFR inhibitor resistance mechanisms in lung cancer patients. Nature Commun 2016;7:1–15.
18. Mok T, Wu Y-L, Lee JS, Yu C-J, Sriuranpong V, Sandoval-Tan J, et al. Detection and dynamic changes of EGFR mutations from circulating tumor DNA as a predictor of survival outcomes in NSCLC patients treated with first-line intercalated erlotinib and chemotherapy. Clin Cancer Res 2015;21:3196–203.
19. Guibert N, Pradines A, Farella M, Casanova A, Gouin S, Keller L, et al. Monitoring KRAS mutations in circulating DNA and tumor cells using digital droplet PCR during treatment of KRAS-mutated lung adenocarcinoma. Lung Cancer 2016;100:1–4.
20. Takahama T, Azuma K, Shimokawa M, Takeda M, Ishii H, Kato T, et al. Plasma screening for the T790M mutation of EGFR and phase 2 study of osimertinib efficacy in plasma T790M–positive non–small cell lung cancer: West Japan Oncology Group 8815L/LPS study. Cancer 2020;126:1940–8.
21. Forshew T, Murtaza M, Parkinson C, Gale D, Tsui DWY, Kaper F, et al. Noninvasive identification and monitoring of cancer mutations by targeted deep sequencing of plasma DNA. Sci Transl Med 2012;4:136ra68.
22. Diehl F, Schmidt K, Choti MA, Romans K, Goodman S, Li M, et al. Circulating mutant DNA to assess tumor dynamics. Nat Med 2008;14:985–90.
23. Marchetti A, Palma JF, Felicioni L, De Pas TM, Chiari R, Del Grammastro M, et al. Early prediction of response to tyrosine kinase inhibitors by quantification of EGFR mutations in plasma of NSCLC Patients. J Thorac Oncol 2015;10:1437–43.
24. Phallen J, Sausen M, Adleff V, Leal A, Hruban C, White J, et al. Direct detection of early-stage cancers using circulating tumor DNA. Sci Transl Med 2017;9: eaan2415.
25. Douillard J-Y, Ostoros G, Cobo M, Ciuleanu T, Cole R, McWalter G, et al. Gefitinib treatment in EGFR mutated Caucasian NSCLC: circulating-free tumor DNA as a surrogate for determination of EGFR Status. J Thorac Oncol 2014;9:1345–53.
26. Zhu G, Ye X, Dong Z, Lu YC, Sun Y, Liu Y, et al. Highly sensitive droplet digital PCR method for detection of EGFR-activating mutations in plasma cell–free DNA from patients with advanced non–small cell lung cancer. J Mol Diagn 2015;17:265–72.
27. Clark TA, Chung JH, Kennedy M, Hughes JD, Chennagiri N, Lieber DS, et al. Analytical validation of a hybrid capture–based next-generation sequencing clinical assay for genomic profiling of cell-free circulating tumor DNA. J Mol Diagn 2018;20:686–702.
28. Chabon JJ, Hamilton EG, Kurtz DM, Esfahani MS, Moding EJ, Stehr H, et al. Integrating genomic features for non-invasive early lung cancer detection. Nature 2020;580:245–51.
29. Martins VC, Cardoso FA, Germano J, Cardoso S, Sousa L, Piedade M, et al. Femtomolar limit of detection with a magnetoresistive biochip. Biosens Bioelectron 2009;24: 2690–5.
30. Tamanaha CR, Mulvaney SP, Rife JC, Whitman LJ. Magnetic labeling, detection, and system integration. Biosens Bioelectron 2008;24:1–13.
31. Lee J-R, Haddon DJ, Wand HE, Price JV, Diep VK, Hall DA, et al. Multiplex giant magnetoresistive biosensor microarrays identify interferon-associated autoantibodies in systemic lupus erythematosus. Sci Rep 2016;6: 27623.
32. Gaster RS, Hall DA, Nielsen CH, Osterfeld SJ, Yu H, Mach KE, et al. Matrix-insensitive protein assays push the limits of biosensors in medicine. Nat Med 2009;15: 1327–32.
33. Gani AW, Wei W, Shi R-Z, Ng E, Nguyen M, Chua M-S, et al. An automated, quantitative, and multiplexed assay suitable for point-of-care hepatitis B. Sci Rep 2019;9: 1–11.
34. Edelstein RL, Tamanaha CR, Sheehan PE, Miller MM, Baselt DR, Whitman LJ, et al. The BARC biosensor applied to the detection of biological warfare agents. Biosens Bioelectron 2000;14:805–13.
35. Koets M, van der Wijk T, van Eemeren JTWM, van Amerongen A, Prins MWJ. Rapid DNA multi-analyte immunoassay on a magneto-resistance biosensor. Biosens Bioelectron 2009;24:1893–8.
36. Rizzi G, Dufva M, Hansen MF. Two-dimensional salt and temperature DNA denaturation analysis using a magnetoresistive sensor. Lab Chip 2017;17:2256–63.
37. Rizzi G, Westergaard Østerberg F, Dufva M, Fougt Hansen M. Magnetoresistive sensor for real-time single nucleotide polymorphism genotyping. Biosens Bioelectron 2014;52:445–51.
38. Rizzi G, Lee J-R, Dahl C, Guldberg P, Dufva M, Wang SX, et al. Simultaneous profiling of DNA mutation and methylation by melting analysis using magnetoresistive biosensor array. ACS Nano 2017;11: 8864–70.
39. Nesvet J, Rizzi G, Wang SX. Highly sensitive detection of DNA hypermethylation in melanoma cancer cells. Biosens Bioelectron 2019;124–125:136–42.
40. Schøler LV, Reinert T, Ørntoft M-BW, Kassentoft CG, Árnadóttir SS, Vang S, et al. Clinical implications of monitoring circulating tumor DNA in patients with colorectal cancer. Clin Cancer Res 2017;23:5437–45.